

A Datta-Das transistor with enhanced spin control

J. Carlos Egues^{a)}, Guido Burkard, and Daniel Loss

Department of Physics and Astronomy, University of Basel,

Klingelbergstrasse 82, CH-4056 Basel, Switzerland

(Dated: February 1, 2008)

We consider a two-channel spin transistor with weak spin-orbit induced interband coupling. We show that the coherent transfer of carriers between the coupled channels gives rise to an *additional* spin rotation. We calculate the corresponding spin-resolved current in a Datta-Das geometry and show that a weak interband mixing leads to enhanced spin control.

PACS numbers: 71.70.Ej,72.25.-b,73.23.-b,73.63.Nm

arXiv:cond-mat/0209682v2 [cond-mat.mes-hall] 17 Apr 2003

^{a)}Also at: Department of Physics and Informatics, University of São Paulo at São Carlos, 13560-970 São Carlos/SP, Brazil; electronic mail: egues@if.sc.usp.br

The pioneering spin-transistor proposal of Datta and Das [1] best exemplifies the relevance of electrical control of magnetic degrees of freedom as a means of spin modulating charge flow. In this device [2], a spin-polarized current [3, 4] injected from the source is spin modulated on its way to the drain via the Rashba spin-orbit [5] (s-o) interaction, Fig. 1(a). The spin transistor operation relies on gate controlling [6] the strength α of the Rashba interaction which has the form $H_R = i\alpha\sigma_y\partial/\partial x$ in a strictly 1D channel [5]. Upon crossing the Rashba-active region of length L , a spin-up incoming electron emerges in the spin-rotated state

$$\begin{pmatrix} 1 \\ 0 \end{pmatrix} \rightarrow \begin{pmatrix} \cos(\theta_R/2) \\ -\sin(\theta_R/2) \end{pmatrix}, \quad (1)$$

where $\theta_R = 2m^*\alpha L/\hbar^2 \equiv 2k_R L$ is the rotation angle and m^* is the electron effective mass [1]. The corresponding spin-resolved conductance is found to be $G_{\uparrow,\downarrow} = e^2(1 \pm \cos \theta_R)/h$.

Here we extend the above picture by considering a geometry with two weakly-coupled Rashba bands in the quasi-one-dimensional channel, Fig. 1(b). We treat the degenerate k states near the band crossings perturbatively in analogy to the nearly-free electron model [7]. This approach allows for a simple analytical description of the problem. We calculate the spin-resolved current by extending the usual procedure of Datta and Das [1] to account for weakly coupled bands. Our main finding is an *additional* spin rotation for injected electrons with energies near the band crossing [see shaded region around ε_F in Fig. 2]. As we derive later on, an incoming spin up electron in channel a emerges from the Rashba region in the rotated state

$$\begin{pmatrix} 1 \\ 0 \\ 0 \\ 0 \end{pmatrix} \rightarrow \frac{1}{2} \begin{pmatrix} \cos(\theta_d/2)e^{-ik_R L} + e^{ik_R L} \\ -i \cos(\theta_d/2)e^{-ik_R L} + ie^{ik_R L} \\ -i \sin(\theta_d/2)e^{-ik_R L} \\ \sin(\theta_d/2)e^{-ik_R L} \end{pmatrix}, \quad (2)$$

where $\theta_d = \theta_R d/k_c$ is the additional spin rotation angle, d the interband matrix element and k_c the wave vector at the band crossing, Fig. 2. From (2) we can find the new spin-resolved conductance

$$G_{\uparrow,\downarrow} = \frac{e^2}{h} \begin{pmatrix} 1 + \cos(\theta_d/2) \cos \theta_R \\ 1 - \cos(\theta_d/2) \cos \theta_R \end{pmatrix}. \quad (3)$$

We now proceed to derive Eqs (2) and (3).

Model. We consider a quasi-one-dimensional wire of length L with two bands a and b described by $\varepsilon_{n,\sigma_z}(k) = \hbar^2 k^2/2m^* + \epsilon_n$, $n = a, b$ and eigenfunctions $\varphi_{k,n,\sigma}(x, y) = e^{ikx} \phi_n(y)|\sigma\rangle/\sqrt{L}$, $\sigma = \uparrow, \downarrow$

where the $\phi_n(y)$'s denote the transverse confinement wave functions. In the presence of the Rashba s-o interaction, we can derive a Hamiltonian for the system in the basis of the uncoupled wave functions $\{\varphi_{k,n,\sigma_z}(x,y)\}$. This reads,

$$H_R = \begin{bmatrix} \varepsilon_+^a(k) & 0 & 0 & -\alpha d \\ 0 & \varepsilon_-^a(k) & \alpha d & 0 \\ 0 & \alpha d & \varepsilon_+^b(k) & 0 \\ -\alpha d & 0 & 0 & \varepsilon_-^b(k) \end{bmatrix}, \quad (4)$$

where $d \equiv \langle \phi_a(y) | \partial/\partial y | \phi_b(y) \rangle$, $\varepsilon_s^n(k) = \hbar^2(k - sk_R)^2/2m^* + \epsilon_n - \epsilon_R$, $\epsilon_R \equiv \hbar^2 k_R^2/2m^*$, ($s = \pm$, $n = a, b$) and we have considered $|\sigma\rangle$ to be the eigenbasis of σ_y . For $d = 0$ the Hamiltonian in (4) is diagonal and yields uncoupled Rashba dispersions $\varepsilon_s^n(k)$ (thin lines in Fig. 2); the corresponding wave functions are $\varphi_{k,n,s}(x,y)$ (here $|\sigma\rangle \rightarrow |s = \pm\rangle = [|\uparrow\rangle \pm i|\downarrow\rangle]/\sqrt{2}$). Note that for $d = 0$ the bands cross for some values of k . For instance, for $k > 0$ a crossing occurs at $k_c = (\epsilon_b - \epsilon_a)/2\alpha$. For non-zero interband coupling $d \neq 0$ [8], we can diagonalize H_R exactly (see Mireles and Kirczenow in Ref. [8]) to find the new dispersions (thick lines in Fig. 2).

Bands near k_c . Since we are interested in transport with injection energies near the crossing, we follow below a simpler perturbative approach [7] to determine the energy dispersions and wave functions near k_c . Near the crossing we can solve the reduced Hamiltonian

$$\tilde{H}_R = \begin{bmatrix} \varepsilon_-^a(k) & \alpha d \\ \alpha d & \varepsilon_+^b(k) \end{bmatrix}, \quad (5)$$

which to lowest order yields

$$\varepsilon_{\pm}^{\text{approx}}(k) = \frac{\hbar^2 k^2}{2m^*} + \frac{1}{2}\epsilon_b + \frac{1}{2}\epsilon_a \pm \alpha d. \quad (6)$$

As shown in the inset of Fig. 2, Eq. (6) describes very well the anti-crossing of the bands near k_c . The corresponding *zero-order* eigenstates are

$$|\psi_{\pm}\rangle = \frac{1}{\sqrt{2}} [|-\rangle_a \pm |+\rangle_b] = \frac{1}{\sqrt{2}} \left[\begin{pmatrix} 1 \\ -i \end{pmatrix}_a \pm \begin{pmatrix} 1 \\ i \end{pmatrix}_b \right], \quad (7)$$

where the sub-indices indicate the respective channel. The analytical form in (6) allows us to determine the wave vectors k_{c1} and k_{c2} in Fig. 2 straightforwardly: we assume $k_{c1} = k_c - \Delta/2$ and $k_{c2} = k_c + \Delta/2$ and solve $\varepsilon_+^{\text{approx}}(k_{c1}) = \varepsilon_-^{\text{approx}}(k_{c2})$ (assumed $\sim \varepsilon_F$) to find

$$\Delta = \frac{2m^* \alpha d}{\hbar^2 k_c} = 2 \frac{k_R}{k_c} d. \quad (8)$$

Note that to the lowest order used here the horizontal splitting Δ is constant and symmetric about k_c .

Boundary conditions. We now consider a spin-up electron entering the Rashba-active region of length L in the wire. Following the usual approach, we expand this incoming state in terms of the coupled Rashba states in the wire. We consider only the states k_{c1} , k_{c2} , and k_2 in the expansion

$$|\Psi\rangle = \frac{1}{2}|\psi_+\rangle e^{ik_{c1}x} + \frac{1}{2}|\psi_-\rangle e^{ik_{c2}x} + \frac{1}{\sqrt{2}}|+\rangle_a e^{ik_2x}. \quad (9)$$

The above *ansatz* satisfies the boundary conditions for both the wave function and (to leading order) its derivative $x = 0$. More explicitly, the velocity operator condition [10] at $x = 0$ for an electron with $k = k_F$ yields

$$\begin{pmatrix} k_F \\ 0 \\ 0 \\ 0 \end{pmatrix} = \frac{1}{2} \begin{pmatrix} k_c + k_2 \\ -i(k_c - k_2 - 2k_R) \\ -\Delta/2 \\ -i\Delta/2 \end{pmatrix} = \frac{1}{2} \begin{pmatrix} k_c + k_2 \\ 0 \\ -\Delta/2 \\ -i\Delta/2 \end{pmatrix}, \quad (10)$$

where we used $k_2 - k_c = 2k_R$ (still valid to leading order). The ‘four-vector’ notation in (10) concisely specifies the spin states in channels a (upper half) and b (lower half). Note that Eq. (10) is satisfied provided that $\Delta \ll 4k_F$. This inequality is satisfied in our system for realistic parameters.

Underlying the *ansatz* in (9) is the assumption of unity transmission through the Rashba region. Here we have in mind the particular spin-transistor geometry sketched in Fig. 1(a): a gate-controlled Rashba-active region of extension L *smaller* than the total length L_0 of the wire. In this configuration, there are only small band offsets (which we neglect) of the order of $\epsilon_R \ll \epsilon_F$ at the entrance ($x = 0$) and exit ($x = L$) of the Rashba region. Hence transmission is indeed very close to unity, see Ref. [9]. The boundary conditions at $x = L$ are also satisfied.

Generalized spin-rotated state. From Eq. (9) we find that a spin-up electron entering the Rashba

region at $x = 0$ emerges from it at $x = L$ in the spin-rotated state

$$\begin{aligned} \Psi_{\uparrow,L} &= \frac{1}{4} \left[\begin{pmatrix} e^{-iL\Delta/2} \\ -ie^{-iL\Delta/2} \\ e^{-iL\Delta/2} \\ ie^{-iL\Delta/2} \end{pmatrix} + \begin{pmatrix} e^{iL\Delta/2} \\ -ie^{iL\Delta/2} \\ -e^{iL\Delta/2} \\ -ie^{iL\Delta/2} \end{pmatrix} \right] e^{ik_c L} + \frac{1}{2} \begin{pmatrix} 1 \\ i \\ 0 \\ 0 \end{pmatrix} e^{ik_2 L} \\ &= \frac{1}{2} e^{i(k_c+k_R)L} \begin{pmatrix} \cos(\theta_d/2)e^{-ik_R L} + e^{ik_R L} \\ -i \cos(\theta_d/2)e^{-ik_R L} + ie^{ik_R L} \\ -i \sin(\theta_d/2)e^{-ik_R L} \\ \sin(\theta_d/2)e^{-ik_R L} \end{pmatrix}, \end{aligned} \quad (11)$$

which is essentially Eq. (2). Observe that in absence of interband coupling (i.e., $\theta_d = 0$) Eq. (11) reduces to the Datta-Das state in (1). An expression similar to (11) holds for the case of an incoming spin-down electron.

Spin-resolved current. For $x \geq L$ we have

$$\begin{aligned} \Psi_{\uparrow}(x \geq L, y) &= \frac{1}{2} \begin{pmatrix} e^{-i\theta_R/2} \cos(\theta_d/2) + e^{i\theta_R/2} \\ -ie^{-i\theta_R/2} \cos(\theta_d/2) + ie^{i\theta_R/2} \end{pmatrix} e^{i(k_c+k_R)x} \phi_a(y) + \\ &\quad \frac{1}{2} \begin{pmatrix} -ie^{i\theta_R/2} \sin(\theta_d/2) \\ e^{i\theta_R/2} \sin(\theta_d/2) \end{pmatrix} e^{i(k_c-k_R)x} \phi_b(y), \end{aligned} \quad (12)$$

which describes plane waves in the *uncoupled* channels a and b arising for an incoming spin-up electron in channel a . The total current follows straightforwardly (Landauer-Büttiker) from Eq. (12)

$$I_{\uparrow,\downarrow} = \frac{e}{h} eV [1 \pm \cos(\theta_d/2) \cos \theta_R]. \quad (13)$$

where $eV \ll \varepsilon_F$ is the applied bias between the source and drain. The spin-dependent conductance in (3) follows immediately from (13). Equation (13) clearly shows the additional modulation θ_d of the spin-resolved current due to s-o induced interband coupling. Figure 3 illustrates the angular dependence of G_{\downarrow} as a function of θ_R and θ_d . The s-o mixing angle θ_d enhances the possibilities for spin control in the Datta-Das transistor.

Realistic parameters. For concreteness, let us consider infinite transverse confinement (width w). In this case, $\varepsilon_b - \varepsilon_a = 3\hbar^2\pi^2/2mw^2$ and the interband coupling constant $d = 8/3w$. We choose $\varepsilon_b - \varepsilon_a = 16\varepsilon_R$, which implies (i) $\alpha = (\sqrt{3}\pi/4)\hbar^2/mw = 3.45 \times 10^{-11}$ eVm (and $\varepsilon_R \sim 0.39$ meV) for $m = 0.05m_0$ and $w = 60$ nm, (ii) $\varepsilon(k_c) = 24\varepsilon_R$ [ε_F should be tuned to $\sim \varepsilon(k_c)$], and

(iii) $k_c = 8\epsilon_R/\alpha$. Assuming $L = 69$ nm [Rashba region length, Fig. 1(a)], we find $\theta_R = \pi$ and $\theta_d = \theta_R d/k_c = \pi/2$, since $d/k_c \sim 0.5$. This is a conservative estimate. In principle, θ_d can be varied independently of θ_R via lateral gates which alter w . Note also that $\Delta/4k_F \sim 0.05$ [validity of Eq. (10)] for the above parameters. Finally, we note that the most relevant spin-flip mechanism (Dyakonov-Perel) should be suppressed in quasi-one-dimensional systems such as ours [11]. In addition, thermal effects are irrelevant in the experimentally feasible linear regime [12] we consider here

This work was supported by NCCR Nanoscience, the Swiss NSF, DARPA, and ARO. We acknowledge useful discussions with D. Saraga.

List of references

- [1] S. Datta and B. Das, *Appl. Phys. Lett.* **56**, 665 (1990).
- [2] G. Meir, T. Matsuyama, and U. Merkt, *Phys. Rev. B* **65**, 125327 (2002); C.-M. Hu, J. Nitta, A. Jensen, J. B. Hansen, H. Takayanagi, T. Matsuyama, D. Heitmann, and U. Merkt, *J. Appl. Phys.* **91**, 7251 (2002).
- [3] R. Fiederling, M. Keim, G. Reuscher, W. Ossau, G. Schmidt, A. Waag, L. W. Molenkamp, *Nature* **402**, 787 (1999); Y. Ohno, D. K. Young, B. Beschoten, F. Matsukura, H. Ohno, D. D. Awschalom, *Nature* **402**, 790 (1999).
- [4] J. C. Egues, *Phys. Rev. Lett.* **80**, 4578 (1998).
- [5] Yu. A. Bychkov and E. I. Rashba, *JETP Lett.* **39**, 78 (1984).
- [6] J. Nitta T. Akazaki, H. Takayanagi, and T. Enoki, *Phys. Rev. Lett.* **78**, 1335 (1997); G. Engels, J. Lange, Th. Schäpers, and H. Lüth, *Phys. Rev. B* **55**, R1958 (1997); D. Grundler, *Phys. Rev. Lett.* **84**, 6074 (2000); Y. sato, T. Kita, S. Gozu, and S. Yamada, *J. Appl. Phys.* **89**, 8017 (2001).
- [7] N. W. Ashcroft and N. D. Mermin, *Solid State Physics*, Ch. 9. (Holt, Rinehart, and Winston, New York, 1976).
- [8] A. V. Moroz and C. H. W. Barnes, *Phys. Rev. B* **60**, 14272 (1999); F. Mireles and G. Kirczenow, *Phys. Rev. B* **64**, 024426 (2001); M. Governale and U. Zülicke, *Phys. Rev. B* **66**, 073311 (2002).
- [9] J. C. Egues, G. Burkard, and D. Loss, *Phys. Rev. Lett.* **89**, 176401 (2002).
- [10] E. A. de Andrada e Silva, G. C. La Rocca, and F. Bassani, *Phys. Rev. B* **55**, 16293 (1997); L. W. Molenkamp, G. Schmidt, and G.E.W. Bauer, *Phys. Rev. B* **64**, R121202 (2001).
- [11] A. Bournel, P. Dollfus, P. Bruno, and P. Hesto, *Eur. Phys. J. AP* **4**, 1 (1998).
- [12] S. Datta, *Electronic transport in mesoscopic systems* (Cambridge University Press, Cambridge, 1997), Ch. 2, p. 89.

Figures



FIG. 1: Spin transistor geometry with a two-band channel. (a) The length L of the Rashba region is smaller than the total length L_0 of the wire. (b) Sketch of energy dispersions in the s-o active region with and without interband coupling (Rashba bands) and away from it (parabolic bands). Note the small band offsets between adjacent regions in the wire.

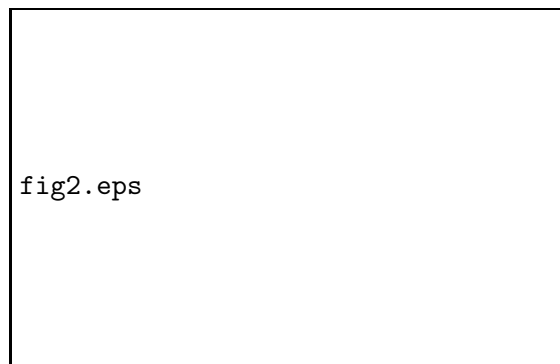


FIG. 2: Band structure in the presence of spin-orbit coupling. In absence of interband mixing the Rashba dispersions are uncoupled (thin solid lines) and cross at, e.g., k_c . For non-zero interband coupling the bands anti cross (thick solid lines). The inset shows a blowup of the dispersion region near the crossing: the approximate solution [dotted lines, perturbative approach, Eq. (6)] describes well the energy dispersions near k_c .



FIG. 3: Angular dependence of the spin-down conductance. The additional modulation θ_d due to s-o interband mixing and θ_R can be varied independently.

